Experimental investigations on the nonlinear dynamics and chaos bandwidth of a monolithically integrated semiconductor laser subject to optical injection

Zhu-Qiang Zhong†, Zheng-Mao Wu†, Ling-Juan Zhao‡, Dan Lu‡, Wan-Qing Zhu†, Xue-Mei Yin†, and Guang-Qiong Xia†,*

†School of Physical Science and Technology, Southwest University, Chongqing 400715, China
‡Key Laboratory of Semiconductor Materials Science, Institute of Semiconductors, Chinese Academy of Science, Beijing 100083, China
*Email: gqxia@swu.edu.cn

Abstract–The nonlinear dynamics and chaos bandwidth of a three-section monolithically integrated semiconductor laser (MISL) subject to optical injection are investigated experimentally. The results show that, the solitary MISL can operate at various dynamical states by adjusting the currents of three sections, but the chaotic region is very small and the maximum chaos bandwidth is about 14 GHz. After introducing an external optical injection, mappings of the dynamical states and the chaos bandwidth of the MISL in the parameter space of the injection strength and frequency detuning are presented. Under suitable injection parameters, the chaotic region can be greatly expanded, and the chaos bandwidth can reach more than 36 GHz.

1. Introduction

In recent years, photonic integrated circuits (PICs) developed very fast for its lower cost, more compact and better reproducibility for mass production compared with discrete optical components [1]-[3]. Monolithically integrated semiconductor lasers (MISLs) [4]-[15], as one kind of PICs, have attracted intensive attention due to their unique virtues. Through specific design and manufacture, MISLs can output different dynamical states [4]-[6] and apply to various applications such as chaos synchronization [7], [8] and clock recovery [9], high-speed physical random bit generation [10] and high-quality microwave generation [11]. Since the 1990s, the nonlinear dynamics of MISLs had been investigated [12]-[14]. Recently, we reported the route into and out of chaos in a three-section MISL, and obtained high-dimensional chaos output [15].

Due to the restriction by the relaxation oscillation frequency of the DFB section in a MISL, the bandwidth of the chaos output from a solitary MISL is usually at a level of 10 GHz [6], [10], which sometimes may not meet the requirements in some special applications such as over 10 Gb/s high-speed optical chaotic communication and ultra-high-speed random number generation. Optical injection, known as a common perturbation, is generally introduced to a semiconductor laser to provide an external degree of freedom, thus various dynamics can be obtained, including stable and unstable injection locking, four-wave mixing, instabilities and chaos [16]. Especially, the bandwidth of chaos output can be greatly enhanced by optical injection [17], [18]. Based on above considerations, in this work, we experimentally investigate the dynamics and chaos bandwidth of a MISL subject to optical injection.

2. Experimental Setup

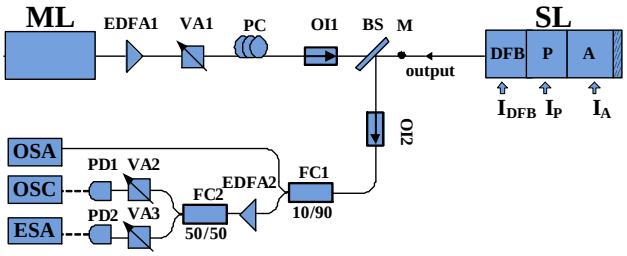

Fig. 1. Experimental setup. Solid lines: optical paths; dashed lines: electrical paths. ML: master laser; SL: slave laser; EDFA: erbium doped fiber amplifier; VA: variable attenuator; FC: fiber coupler; PM: power meter; PC: polarization controller; OI: optical isolator; BS: beam splitter; DFB: distributed feedback section; P: phase section; A: amplifier section; PD: photo-detector; ESA: electrical spectrum analyzer; OSC: oscilloscope; OSA: optical spectrum analyzer; M: measuring point.

Figure 1 shows the experimental setup. A tunable laser source is utilized as the master laser (ML) to provide optical injection. The slave laser (SL) is a three-section MISL, which is designed and fabricated by ourselves [15] and is composed of a distributed feedback (DFB) section, a phase (P) section and an amplifier (A) section with the currents of three sections are labeled as I_{DFB}, I_P and I_A, respectively. During total experimental process, the temperature of the MISL is stabilized at 18.54 ℃.

The output of ML firstly passes through an erbium doped fiber amplifier (EDFA1), a polarization controller (PC), an optical isolator (OI1), a beam splitter (BS), and then injects into the SL. A variable attenuator (VA1) is used to adjust the injection power. The output from the left facet of MISL passes through BS, OI2, and then is divided into two parts by FC1. One part with relatively low power is sent to an optical spectrum analyzer. The other part with relatively high power is amplified by EDFA2 firstly and then divided into two parts, which are transferred into two electronic signals by two fast photo-detectors (PDs), respectively. One electronic signal is sent to an oscilloscope for observing the time series of the

MISL output, and the other is sent to an electrical spectrum analyzer for analyzing the power spectra of the MISL output signal. M is the measuring point for monitoring the output power of the solitary MISL and the injection optical power.

3. Results and discussion

3.1. MISL without Optical Injection

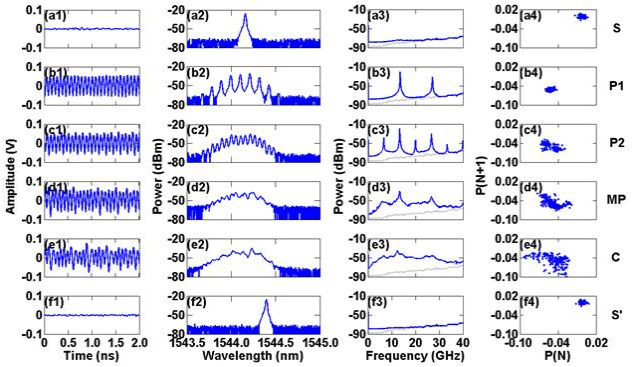

Fig. 2. Time series, optical spectra, power spectra, and phase portraits of typical dynamical states output from the solitary MISL under different I_A for I_{DFB} = 70.00 mA and I_p =34.00 mA, where from top to bottom I_A is (a) 10.00 mA, (b) 18.15 mA, (c) 19.91 mA, (d) 21.70 mA, (e) 23.58 mA, and (f) 27.50 mA, respectively. The gray lines in power spectra denote the noise floor.

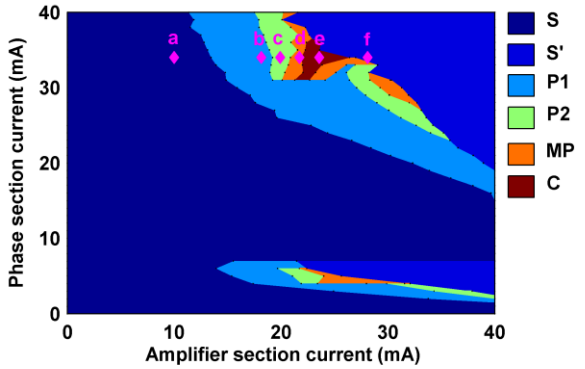

Fig. 3. Mapping of the dynamical states of the solitary MISL in the parameter space of I_P and I_A, where different colors denote different states. The points a-f, corresponding to the case of row a-f in Fig. 2, respectively.

Figure 2 shows the time series, optical spectra, power spectra, and phase portraits of the output from the solitary MISL under different I_A for I_{DFB}=70.00 mA and I_P = 34.00 mA. For I_A=10.00 mA, the output power is nearly a constant with small ripples due to the noise, the optical spectrum is a typical single mode shape, the power spectrum is similar to the noise floor, and the phase portrait is an extended dot. Therefore, the dynamical state of the solitary MISL can be determined to be a stable state (S). For I_A=18.15 mA, the time series shows a periodic oscillation, whose fundamental frequency is close to the relaxation oscillation frequency and is about 13.511 GHz obtained from the power spectrum, and the phase portrait is a dense dot. Therefore, it can be identified that the dynamical state is a period one state (P1). For I_A=19.91 mA, both the sub-harmonic frequency and fundamental frequency present clearly, which is the typical characteristics of doubled periodicity, and then the dynamics could be identified as a period two state (P2). Increasing I_A to 21.70 mA, some new frequencies emerge around the fundamental frequency and sub-harmonic frequency, which is the feature of multi-period state (MP). For I_A = 23.58 mA, the time series is a noise-like waveform, a broad and smooth power spectral distribution could be observed and the phase portrait shows a widely scattered distribution over a large area. All these features indicate that the solitary MISL operates at a chaotic state (C). Further increasing I_A to 27.50 mA, a mode hopping occurs and the dynamics of solitary MISL returns to a stable state. In order to distinguish the two stable states when I_A = 10.00 mA and I_A = 27.50 mA, the stable state after mode hopping is named as S'. In a word, a route of S-P1-P2-MP-C-S' is presented under I_{DFB} = 70.00 mA and I_P = 34.00 mA through scanning I_A.

Figure 3 integrates a mapping of the dynamic states in the parameter space of I_P and I_A. The marked points a-f correspond to the case of Fig. 2(a)-(f), respectively. For relatively low I_A, the MISL keeps a stable state. When I_p is about 34.00 mA, various dynamical states can be observed with the increase of I_A. Here, we introduce the effective bandwidth [19] to evaluate the chaotic bandwidth of the chaotic region in Fig. 3 though the region that the solitary MISL operates at chaotic state is small.

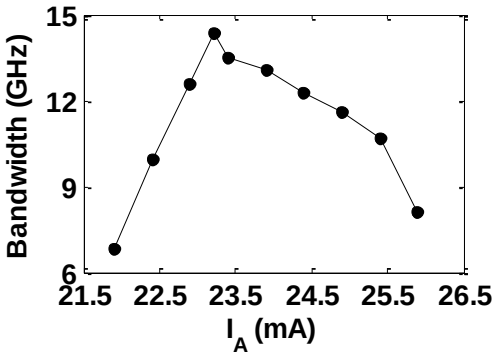

Fig. 4. Variations of chaotic bandwidth with I_A for I_{DFB} = 70.00 mA and I_P = 34.00 mA.

Fig. 4 displays the chaotic bandwidth as a function of I_A for I_{DFB} and I_P are fixed at 70.00 mA and 34.00 mA, respectively. As shown in this diagram, with the increase of I_A from 21.90 mA to 25.90 mA, the chaotic bandwidth increases firstly, after reaches a maximum of 14.36 GHz for I_A = 23.22 mA, and then decreases. Our related experimental results show that 14.36 GHz is approximately maximal chaotic bandwidth within the chaotic region. Therefore, we fix I_{DFB}, I_P, and I_A at 70.00 mA, 34.00 mA, and 23.22 mA, respectively, and then investigate how the introduction of optical injection affects the effective bandwidth.

3.2. MISL with Optical Injection

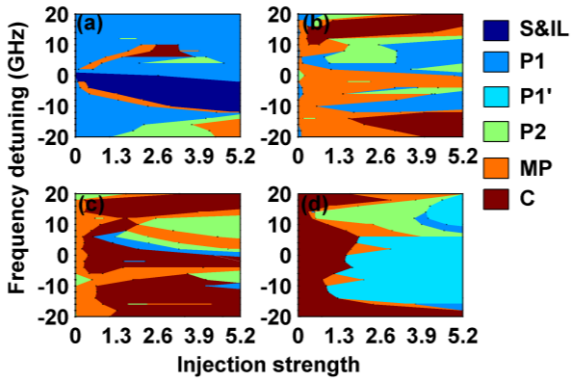

Fig. 5. Dynamical states of a MISL subjected to external optical injection in the parameter space of injection strength and frequency detuning, where the operation parameters of MISL for (a)-(d) correspond to points a, b, c and e in Fig. 3, respectively.

We select four different operation points (points a, b, c, and e in Fig. 3) to explore the influence of external optical injection on the dynamics of the MISL, and the corresponding results are shown in Fig. 5(a)-(d), respectively. The injection strength K_{in} is defined as the ratio of the injection power and output power of the solitary MISL measured at point M in Fig. 1. For the operation point a, the solitary MISL originally operates at a stable state. However, as shown in Fig. 5(a), after introducing an external optical injection, a large region of injection locking (IL) located at negative frequency detuning can be observed, in which the MISL under optical injection maintain a stable state. In other injection parameters, the dynamical state of the MISL transfers into other dynamical states including P1, P2, MP and the chaotic state emerges in the region with positive frequency detuning. Figure 5(b) shows the corresponding result for I_A = 18.15 mA (operation point b). When external optical injection introduced, though P1 can also be observed, some new dynamical states such as P2, MP, and chaos appear. Especially, compared with that for the case of I_A = 10.00 mA as shown in Fig. 5(a), two larger chaotic regions can be observed, which locate at positive and negative frequency detuning areas, respectively. For I_A = 19.91 mA and 23.58 mA, the corresponding results are shown in Fig. 5(c) and (d), respectively. It should be specially pointed out that as shown in Fig. 5(d), a new P1 (named as P1' here) different from P1 mentioned above, has been observed, which is originated from the beating between the injection laser and the new mode caused by mode hopping and a large I_A may be helpful to expand the chaotic region. Next, the influence of optical injection on the chaotic bandwidth will be studied.

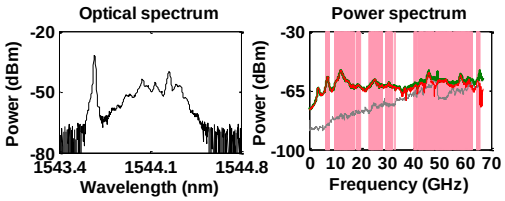

Fig. 6. Optical spectrum (left column) and power spectrum (right column) of the MISL under optical injection with injection ratio K_{in} = 2.88 and frequency detuning Δf = 60.00 GHz, I_{DFB} = 70.00 mA, I_P = 34.00 mA and I_A = 23.22 mA. In power spectrum, the gray, green and red lines denote the noise floor, the measured power spectra, and the power spectrum after subtracting the background noise, respectively. The shaded areas denote the spectral spans that have been counted toward the effective bandwidth.

Figure 6 displays the optical spectrum and the power spectrum of the MISL under optical injection with injection ratio K_{in} = 2.88 and frequency detuning Δf = 60.00 GHz. I_P and I_A are fixed at 34.00 mA and 23.22 mA based on Fig. 4. As shown in Fig. 6, after the optical injection is introduced, the optical spectrum maintains broad but an obvious peak emerges at the frequency of injection light, the power spectrum of is broad and smooth. Further calculation of the effective bandwidth shows that the chaotic bandwidth increases from 14.36 GHz to 36.99 GHz. In the following, the impacts of the injection ratio and the frequency detuning on the chaos bandwidth of chaotic output will be investigated in details.

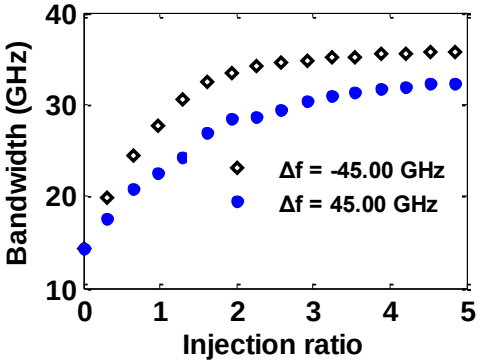

Fig. 7. Chaos bandwidth as a function of the injection ratio K_{in} under Δf = -45.00 GHz and Δf = 45.00 GHz.

Figure 7 displays the chaos bandwidth of chaotic signal from the MISL as a function of injection ratio K_{in} for Δf = -45.00 GHz and Δf = 45.00 GHz. With the increase of K_{in}, the chaos bandwidth rapidly increases firstly, and then slowly increases to a relative stable value. A similar trend can be observed for Δf = -45.00 GHz and Δf = 45.00 GHz. For a larger value of K_{in}, the optical injection may lead a change of dynamical state, and then the variation trend of the bandwidth with the injection ratio will be more complicated.

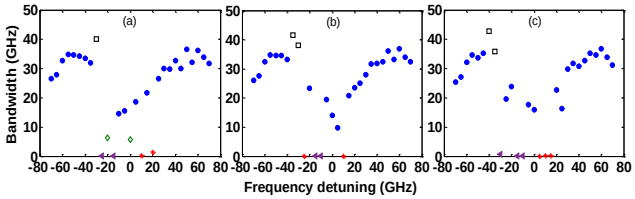

Fig. 8. Effective bandwidth as a function of frequency detuning Δf for different injection ratio, K_{in} = 1.92 (a), K_{in} = 2.88 (b), K_{in} = 3.85 (c). The filled circle, hollow square, hollow rhombus, snowflake, and solid triangle represent chaotic state (C), stable state (S), multi-period oscillation (MP), period-two oscillation (P2) and period-one oscillation (P1), respectively.

Finally, Figure 8 shows the variation of the effective bandwidth with Δf under K_{in} = 1.92 (a), 2.88 (b) and 3.85 (c), respectively. It can be seen that, when the absolute values of Δf are relatively small, P1, P2, MP and chaotic states can be identified with the help of effective bandwidth and the dynamical states are very sensitive to the variation of the frequency detuning. However, for the absolute values of Δf possesses relative large values, the unbroken expanse of chaotic regions can be obtained. For different values of K_{in}, the continuous chaotic regions own different boundaries, and the maximums of the chaos bandwidths are 36.56 GHz under K_{in} = 1.92, 36.99 GHz under K_{in} = 2.88, and 36.86 GHz under K_{in} = 3.85, respectively.

4. Conclusions

In summary, the dynamical characteristics and the chaos bandwidth of a MISL with and without external optical injection have been studied experimentally. The solitary MISL behaves a dynamical route of S-P1-P2-MP-C-S' under I_{DFB} = 70.00 mA and I_P = 34.00 mA through varying I_A. The chaotic region in the parameter space of I_A and I_P is relatively small and the maximal chaos bandwidth is approximately 14 GHz. After introducing external optical injection, the MISL can always be driven into a chaos no matter which state the solitary MISL originally operates at, and a large I_A is helpful to enlarge the chaotic region. The chaos bandwidth can reach more than 36 GHz by selecting suitable injection strength and frequency detuning. We hope this work will be helpful to understand the chaos dynamics of MISLs under optical injection and then exploit their applications in related fields.

Acknowledgments

This work was supported by the National Natural Science Foundation of China under Grant 61178011, Grant 61275116, and Grant 61475127, and the Postgraduate Research and Innovation Project of Chongqing Municipality under Grant no. CYB14054.

References

[1] T. L. Koch, and U. Koren, "Semiconductor photonic integrated circuits," *IEEE J. Quantum Electron.*, vol. 27, pp. 641–653, 1991.

[2] D. Hofstetter, B. Maisenhölder, and H. P. Zappe, "Quantum-well intermixing for fabrication of lasers and photonic integrated circuits," *IEEE J. Sel. Top. Quantum Electron.*, vol. 4, pp. 794–802, 1998.

[3] B. R. Cemlyn, D. Labukhin, I. D. Henning, and M. J. Adams, "Dynamic transitions in a photonic integrated circuit," *IEEE J. Quantum Electron.*, vol. 48, pp. 261-268, 2012.

[4] S. Bauer, O. Brox, J. Kreissl, B. Sartorius, M. Radziunas, J. Sieber, H. J. Wünsche, and F. Henneberger "Nonlinear dynamics of semiconductor lasers with active optical feedback," *Phys. Rev. E*, vol. 69, art. 016206, 2004.

[5] O. Ushakov, S. Bauer, O. Brox, H. J. Wünsche, and F. Henneberger, "Self-organization in semiconductor lasers with ultrashort optical feedback," *Phys. Rev. Lett.*, vol. 92, art. 043902, 2004.

[6] A. Argyris, M. Hamacher, K. E. Chlouverakis, A. Bogris, and D. Syvridis, "Photonic integrated device for chaos applications in communications," *Phys. Rev. Lett.*, vol. 100, art. 194101, 2008.

[7] H. J. Wünsche, S. Bauer, J. Kreissl, O. Ushakov, N. Korneyev, F. Henneberger, E. Wille, H. Erzgräber, M. Peil, W. Elsäßer, and I. Fischer, "Synchronization of delay-coupled oscillators: a study of semiconductor Lasers," *Phys. Rev. Lett.*, vol. 94, art. 163901, 2005.

[8] T. Pérez, M. Radziunas, H. J. Wünsche, C. R. Mirasso, and F. Henneberger, "Synchronization properties of two coupled multisection semiconductor lasers emitting chaotic light," *IEEE Photon. Technol. Lett.*, vol. 18, pp. 2135–2137, 2006.

[9] Y. Sun, J. Q. Pan, L. J. Zhao, W. X. Chen, W. Wang, L. Wang, X. F. Zhao, and C. Y. Lou, "All-optical clock recovery for 20 Gb/s using an amplified feedback DFB Laser," *J. Lightw. Technol.*, vol. 28, pp. 2521–2525, 2010.

[10] R. Takahashi, Y. Akizawa, A. Uchida, T. Harayama, K. Tsuzuki, S. Sunada, K. Arai, K. Yoshimura, and P. Davis, "Fast physical random bit generation with photonic integrated circuits with different external cavity lengths for chaos generation," *Opt. Express*, vol. 22, pp. 11727–11740, 2014.

[11] D. S. Yee, Y. A. Leem, S. B. Kim, D. C. Kim, K. H. Park, S. T. Kim, and B. G. Kim, "Loss-coupled distributed-feedback lasers with amplified optical feedback for optical microwave generation," *Opt. Lett.*, vol. 29, pp. 2243–2245, 2004.

[12] Y. K. Chen and M. C. Wu, "Monolithic colliding-pulse mode-locked quantum-well lasers," *IEEE Quantum Electron.*, vol. 28, pp. 2176-2185, 1992.

[13] T. Franck, S. D. Brorson, A. Moller-Larsen, J. M. Nielsen, and J. Mork, "Synchronization phase diagrams of monolithic colliding pulse-modelocked lasers," *IEEE Photonics Technol. Lett.*, vol. 8, pp. 40-42, 1996.

[14] M. Yousefi, Y. Barbarin, S. Beri, E. A. J. M. Bente, M. K. Smit, R. Nötzel, and D. Lenstra, "New Role for Nonlinear Dynamics and Chaos in Integrated Semiconductor Laser Technology," *Phys. Rev. Lett.*, vol. 98, art. 044101, 2007.

[15] J. G. Wu, L. J. Zhao, Z. M. Wu, D. Lu, X. Tang, Z. Q. Zhong, and G. Q. Xia, "Direct generation of broadband chaos by a monolithic integrated semiconductor laser chip," *Opt. Express*, vol. 21, pp. 23358–23364, 2013.

[16] J. Ohtsubo, Semiconductor Lasers: Stability, Instability and Chaos, third Ed., Springer, Berlin, 2013.

[17] A. B. Wang, Y. C. Wang, and H. C. He, "Enhancing the bandwidth of the optical chaotic signal generated by a semiconductor laser with optical feedback," *IEEE Photonics Technol. Lett.*, vol. 19, pp. 1633-1635, 2008.

[18] Y. Hong, P. S. Spencer, and K. A. Shore, "Enhancement of chaotic signal bandwidth in vertical-cavity surface-emitting laser s with optical injection," *J. Opt. Soc. Am. B: Opt. Phys.*, vol. 29, pp. 415-419, 2012.

[19] F. Y. Lin, Y. K. Chao, and T. C. Wu, "Effective bandwidths of broadband chaotic signals," *IEEE J. Quantum Electron.*, vol. 48, pp. 1010-1014, 2012.